Bioactive Materials 41 (2024) 400–412

Contents lists available at ScienceDirect

Bioactive Materials

journal homepage: www.keaipublishing.com/en/journals/bioactive-materials

Deciphering 3D periodontal fibroblast-macrophage crosstalk in bioactive nanoparticle-guided immunomodulation for treating traumatic dental avulsion

Hadagalu Revana Siddappa Rajeshwari [a], Emily Bishop [b], Aiman Ali [c], Anil Kishen [a,b,d,*]

[a] The Kishen Lab, Dental Research Institute, University of Toronto, Toronto, ON, M5G 1G6, Canada
[b] Faculty of Dentistry, University of Toronto, Toronto, ON, M5G 1G6, Canada
[c] Oral and Maxillofacial Pathology and Oral Medicine, Faculty of Dentistry, University of Toronto, 124 Edward Street, Toronto, Ontario M5G 1G6, Canada
[d] Department of Dentistry, Mount Sinai Health System, Mount Sinai Hospital, Toronto, ON, M5G 1X5, Canada

ARTICLE INFO

Keywords:
Root resorption
Chitosan nanoparticles
Immunomodulation
Periodontal fibroblasts
Macrophages

ABSTRACT

Prolonged extra-oral period in dental avulsion is often associated with loss of viability of Periodontal fibroblasts (PDLF) and increased risk of ankylosis. Root surface treatment with bioactive agents to reduce the risk of ankylosis can be a potential strategy. The objective of the study was to investigate the impact of an engineered chitosan nanoparticles (CSNP), photosensitizer Rose Bengal (RB) functionalized CSNP (CSRB) and sustained dexamethasone (CSDEX) releasing CSNP for application in management of delayed replantation of avulsed teeth. The 3D PDLF-macrophage (Mϕ) collagen model was developed and exposed to LPS, MCSF, RANKL with and without CSDEX/CSNP. Immunofluorescence and cytokine analysis was done at 2 and 7 days to assess cellular interactions. Maxillary right incisors in male Wistar rats were extracted, exposed to extraoral dry or LPS for 1 h and treated with or without CSDEX/CSRB for 1 min before replantation. Rats were euthanized after 21 days for micro-CT, TRAP, and immunofluorescence analysis. CSDEX/CSNP treatment in 3D model significantly reduced CD80, NFATc1, STAT6 and increased CD206 and periostin expression ($p < 0.05$). TNFα, MMP9 was downregulated and IL10, TGFβ1, MMP2 upregulated with CSDEX/CSNP ($p < 0.05$). CSDEX/CSRB in animal study significantly reduced resorption, ankylosis, TRAP activity and osteocalcin expression and increased periostin ($p < 0.05$). CSDEX demonstrated higher anti-inflammatory activity by downregulating TNFα, while CSNP upregulated TGFβ1, periostin, and downregulated MMP9. The combination of matrix stabilization with CSRB with periostin upregulation and sustained releasing CSDEX showed potential for hampering root resorption and ankylosis in dental avulsion.

1. Introduction

Root resorption is a progressive degradation of dentin and cementum, which is the most common negative sequela of tooth avulsion [1]. In traumatic dental injuries involving the unmineralized pre-cementum layer by mechanical or chemical means, the underlying cementum and dentin are exposed to resorptive attack by osteoclasts [2–4]. While osteoclasts are the key resorbing cells, their differentiation from precursor cells macrophages (Mϕ), and the pattern of resorption is spatiotemporally mediated by resident cells in the extracellular matrix and micro-environments [5,6]. Mϕ can polarise either to an inflammatory phenotype (M1) or an alternate phenotype (M2) based on the type of stimuli received, demonstrating plasticity [7]. Mϕ undergoing M1 polarization coalesce to form multinucleated osteoclasts and resorb hard tissues [7].

Periodontal ligament (PDL) is a highly vascular loose connective tissue with PDL fibroblasts (PDLF) as the major cell population, which are embedded in an extracellular matrix (ECM) rich in type I collagen matrix [8]. Type of tissue response in traumatic dental injury avulsion depends on the severity of damage to periodontal tissues and the viability of periodontal fibroblasts (PDLF) [9]. Replacement (32.9 %) and inflammatory (24.1 %) root resorption are the two common type of

Peer review under responsibility of KeAi Communications Co., Ltd.
* Corresponding author. Oral Health Nanomedicine (Tier 1), Dr. Lloyd and Mrs. Kay Chapman Chair in Clinical Sciences, Faculty of Dentistry, University of Toronto, 124 Edward Street, Toronto, Ontario M5G 1G6, Canada.
E-mail address: anil.kishen@dentistry.utoronto.ca (A. Kishen).

https://doi.org/10.1016/j.bioactmat.2024.07.017
Received 12 April 2024; Received in revised form 9 July 2024; Accepted 13 July 2024

tissue response observed in tooth avulsion [9]. Loss of PDLF viability is often accompanied by invasion of bone cells into PDL space resulting in replacement resorption/ankylosis and PDLF on exposure to inflammatory stimuli from pulpal or periodontal origin is associated with inflammatory resorption [4,9–11]. Conventional two-dimensional (2D) monoculture and indirect coculture cell culture models have shown that PDLF when exposed to mechanical force or bacterial lipopolysaccharide (LPS) release proinflammatory mediators that are essential for the clastic differentiation of Mϕ highlighting the paracrine effects [12–14]. Direct coculture models have further emphasized the juxtacrine effects of PDLF on clastic differentiation of Mϕ in resorptive environments [12,15]. While these models provide some insight on cellular interactions in root resorption, it is important to simulate the complex microenvironment that cells encounter in in-vivo condition by providing ECM. In addition to providing structural support, ECM provides diffusion gradient for nutrients and substrate stiffness required for cell proliferation, differentiation, migration, adhesion, and intercellular signaling [16,17]. Lack of three-dimensional (3D) matrix-based models is suggested to impede drug development [18]. Hence, to understand cellular interactions in disease and treatment, it is crucial to develop a 3D collagen-based multicellular coculture model in resorptive environments that simulates in-vivo conditions.

Several restorative materials, with or without antimicrobials, anti-inflammatory agents and biological mediators have been used in the treatment of root resorption. These include calcium hydroxide, doxycycline, dexamethasone, emdogain and platelet rich fibrin [9,19–22] While synthetic agents such as Ca $(OH)_2$ have focused on arresting the root resorption, and antibiotics have focused on reducing microbial burden, it is important to create a microenvironment conducible for favourable healing and generating lost tissue by biological means. Recent advances are focused on the use of biological mediators in root resorption. In addition, synthetic intracanal medicaments such as calcium hydroxide is associated with the necrosis of both resorbing and reparative cells [23]. Hence, there is a need to shift the treatment paradigm in root resorption to enhance healing outcomes.

Enamel matrix protein (Emdogain) is derived from Hertwig's epithelial root sheath of porcine origin which serves as potential biological mediator owing to its role in root formation during the tooth development [24]. Root surface treatment with emdogain not only makes the root more resistant to root resorption but also promotes the formation of new periodontal ligament [20]. However, placement of platelet rich fibrin in the extracted socket in delayed replantation model was not able to provide any significant benefit except reduced inflammatory root resorption [21]. Chitosan is a natural biopolymer derived from chitin that can be synthesized into nanoparticles (NP) [25]. Free hydroxyl and amine group in them makes it possible to functionalize with therapeutic agents to obtain desired treatment benefits [25,26]. Chitosan nanoparticles (CSNP) have been demonstrated to reprogram Mϕ proteomics and cytokine profile to modulate biofilm mediated inflammation. CSNP downregulated IL-1β, nitric oxide and upregulated anti-inflammatory mediators IL-10, TGF-β1. CSNP further promoted PDLF cell viability and migration highlighting its potential in healing process [14,27]. Treatment of LPS contaminated root canal space with photosensitizer (Rose Bengal dye-RB) functionalized CSNP (CSRB) has shown to significantly improve the micro-environment to induce neo-tissue formation and reduce inflammatory resorption [28,29]. Additionally, photodynamically activated CS-RB stabilizes dentin ultrastructure enhancing its mechanical properties and resistance to enzymatic degradation [25,30].

Topical corticosteroids have been assessed in treating avulsed teeth owing to their anti-inflammatory and anti-resorptive potential [22,31]. Dexamethasone is one such potent corticosteroid that have been shown to effectively reduce the degree of inflammatory resorption in avulsed teeth at concentration of 1000 nM but significantly increased the ankylosis [22]. Dexamethasone at a concentration of 16 μg/mL was found to substantially reduce both inflammatory and ankylosis [31]. A sustained dexamethasone releasing chitosan nanoparticles at a concentration of 30 μg/mL was found to induce odontogenic differentiation of stem cells of apical papilla by upregulating ALP gene expression which can be advantageous in treating avulsion injuries [32]. These data emphasize that the anti-clastic and tissue healing effect of dexamethasone is concentration dependant and functionalising it with a biopolymer with sustained release property can be a potential approach to avail its benefits in avulsion. The aim of the current study is to investigate the impact of an engineered chitosan nanoparticles, photosensitizer functionalized chitosan nanoparticles and a sustained dexamethasone releasing chitosan nanoparticles for application in management of root resorption in delayed reimplantation of avulsed teeth. This study will provide valuable insights into a potential treatment option for the predictable treatment of traumatically involved teeth.

2. Materials and methods

Human PDLF were provided as a kind gift from Dr. Douglas Hamilton's lab, Schulich's School of Medicine & Dentistry, London, ON, Canada. Cells were isolated from clinical samples of healthy periodontium. PDLF were cultured in complete DMEM (D5796-Sigma-Aldrich, Canada) with 10 % fetal bovine serum (FBS), 1 % antibiotic/antimycotic at 37 °C in a humidified atmosphere 5 % CO_2. Human acute monocytic leukemia cells (THP-1 monocytes ATCC® TIB-202™ -Rockville, MD, USA) were maintained in complete RPMI 1640 (#R8758, Sigma Aldrich, St. Louis, USA) with 10 % heat inactivated FBS (#19C448, Sigma Aldrich, USA), 1 % antibiotic/antimycotic (#15240-062, Gibco, USA) and 0.1 % β mercaptoethanol (#21985023, Gibco, New York, USA) at 37 °C in a humidified atmosphere with 5 % CO_2. THP-1 cells (2.5×10^5 cells/mL) were differentiated to Mϕ using 60 ng/mL phorbol 12-myristate-13-acetate (PMA-Sigma Aldrich, St. Louis, USA) [27]. Cells from passage 3–5 were used for experiments.

2.1. Experimental method

3D PDLF-Mϕ model was developed using two stage technique (Fig. 1). In stage I, PDLF (4×10^4) suspended in DMEM (100 μL) was mixed with type I bovine collagen (50 μL)(#A1064401 Gibco, ThermoFisher, USA) and 0.1 M sodium hydroxide (7.5 μL). Prepared bioink was seeded into polydimethylsiloxane custome fabricated mold and incubated overnight at 37° C in a humidifying incubator with 5 % CO_2 to allow collagen self-assembly. 3D-PDLF construct was transferred to cell culture well plate containing 1 mL DMEM and incubated for 48h. In stage II, mixture of Mϕ (4×10^5) suspended in DMEM (30 μL), type I bovine collagen (15 μL) and 0.1 M sodium hydroxide (2.25 μL) was seeded on top of 3D-PDLF construct. 3D PDLF-Mϕ coculture received 2 mL DMEM with experimental stimuli [Control: No stimuli, Inflammatory: 1 μg/mL *Porphyromonas gingivalis* lipopolysaccharide (LPS) (#tlrlpglps; InvivoGen, San Diego, CA) [33][31], Resorptive: 30 ng/mL RANKL (#AF-310-01, PeproTech, NJ, USA) and 25 ng/mL M-CSF (#AF-300-25, PeproTech, NJ, USA) [34], Combination (inflammatory + resorptive) with or without CSNP (0.1 mg/mL) or CSNP functionalized with dexamethasone (CSDEX: 30 μg/mL). The cell seeding dentistry [35] and NPs concentrations [27,32] were optimized in the pilot experiments set based on our previous studies. 3D constructs were incubated at 37° C in humidifying incubator with 5 % CO_2 for 7 days and fresh media with respective experimental stimuli and NPs were provided on day 3. Outcome assessment was done at the end of day 2 and day 7 designated as early and late phase of cellular interactions respectively.

2.2. Nanoparticles synthesis

NPs used in the current study were previously synthesized and characterized in our lab. Chitosan was dissolved in 1 v/v% acetic acid solution at a concentration of 0.1 w/v% and pH was adjusted to 5 by

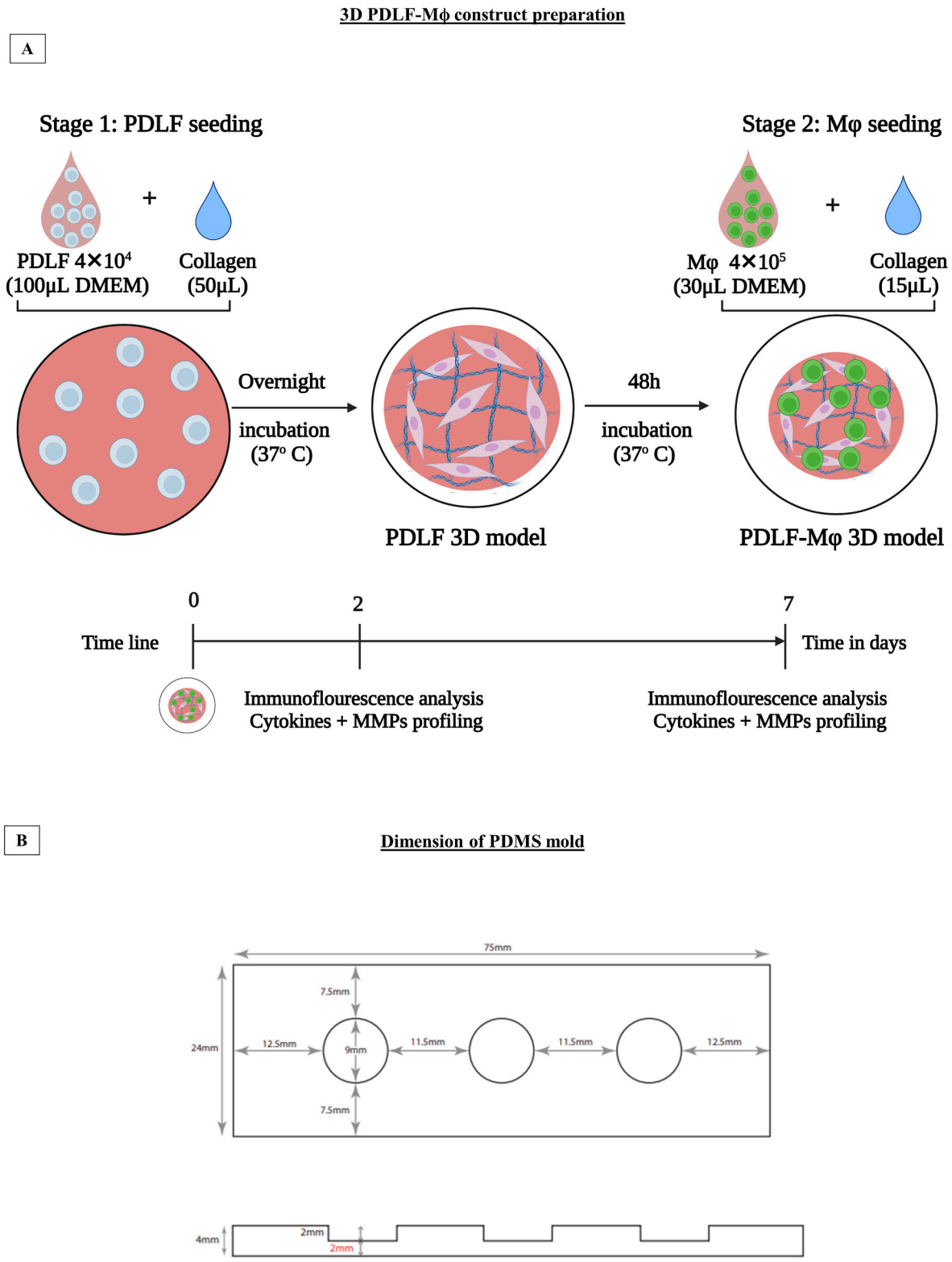

Fig. 1. (A) shows schematic representation of stagewise development of collagen based PDLF-Mϕ 3D model. (B) represents the polydimethylsiloxane (PDMS) mold used for the model development.

adding 1 mol/L NaOH. Prepared chitosan solution was mixed with sodium tripolyphosphate in water 1:3 ratio under stirring at 1000 rpm. CSNP was obtained by centrifugating at 15,000 rpm for 30 min. Following centriguation, residual NaOH was removed by rinsing with deionized water and then freeze-dried. Particle size and zeta potential of CSNP was 93.9 ± 10 nm and 33.9 ± 0.2 mV respectively [36]. For CSRB preparation, CSNP was chemically crosslinked to Rose Bengal using N-ethyl-N′-(3-dimethyl aminopropyl) carbodiimide (EDC 5 mM) and N-Hydroxysuccinimide (NHS 5 mM). Solution of RB (0.05 g) prepared in 10 mL of aqueous EDC (50 mM) was added dropwise to the 1 % chitosan solution over 30 min. The mixture was stirred for 12 h in dark. The CSRB formed were dialyzed (Sigma, cellulose tubing, cut off 12000–14000

g/mol) for 1 week, the filtrate was then freeze-dried starting at −80 °C. Particle size and zeta potential of CSRB was 60 ± 20 nm and 29.9 ± 0.2 mV respectively [25]. For CSDEX, synthesized CSNP (200 mg) was dispersed in ethanol/deionized water (1:1,50 mL) by sonication for 15 min, and 100 mg Dexamethasone dissolved inethanol/deionized water (1:1, 100 mL) was added. After overnight stirring at room temperature, the resultant mixture was centrifuged. Particle size and zeta potential of CSDEX was 112 ± 11 nm and 20.3 ± 3 mV respectively [32,37]. Detailed characterization of these nanoparticles are presented in our previously published papers [32,36].

2.3. Immunofluorescence analysis

Immunofluorescence staining was done to assess the expression of Mϕ markers (CD80,CD206), multinucleation markers (NFATc1, STAT6) and periostin (Table S1). Staining protocol followed was based on our previous study [15]. Formalin fixed cells in 3D-construct were permeabilized with 0.5 % Triton X (T9284-500 ML Sigma-Aldrich, St. Louis MO) and treated with sea block serum free-PBS buffer (#ab166955, Abcam Inc, Cambridge, MA). Cells were stained with fluorophore conjugated antibodies diluted in a sea block serum free-PBS and incubated at 4 °C overnight in the dark. 3D constructs were washed with PBS and counterstained with nuclear stain 40,6-diamidino-2-phenylindole for 5 min. Cells were washed with PBS to remove residual stains and images were captured using confocal laser scanning microscope (Leica SP8 Lightning Confocal/Light Sheet, Leica Microsystems, Richmond, IL, USA). Fluorescence intensity of each marker was assessed based on the intensity sum normalized to the relative volume in the region of interest using Imaris software (Imaris 9.9; Oxford Instruments, Switzerland)

2.4. Cytokine and protease analysis

Cell culture supernatant collected were centrifuged at 10,000×*g* for 5 min and stored at - 80 °C until analysis. A multiplex immunoassay for TNF-α, IL-6, IL-10 [HCYTOMAG-60K-05 HCYTOMAG-60K Milliplex MAP, Millipore, Billerica, MA, USA] and MMP2 and MMP9 [HMMP2MAG-55K-02 Milliplex MAP, Millipore, Billerica, MA, USA] was used. ELISA kit was used to assess TGF-β1 [RAB0460-1 KT Millipore Sigma, Oakville, ON, Canada].

2.5. Animal study

The study protocol was approved by the Ethics Review Board, University of Toronto (#20012802) and protocol follows ARRIVE guidelines 2.0. Fifty-four male Wistar rats (Rattus norvegicus albinus), 6–8 weeks of age, and 150–200g weight were purchased from Charles River Laboratories. Each group had 6 rats, rat species and sample size were chosen as based on previous study [38]. Rats were kept in standard cages with 2–3 rats per cage with standard food and water ad libitum. Rats were anesthetized using Ketamine hydrochloride 75–90 mg/kg and Xylazine 5–10 mg/kg body weight and surgical area was cleaned with 2 % Chlorhexidine Di gluconate. Maxillary right incisor was luxated using winged 1.5 mm Luxator Elevator (Dr. Brett's Pets, Lake Mary, FL. USA) and extracted using curved extraction forceps. Each rat was randomly assigned to PBS, Airdry or LPS (1 μg/mL) exposure for 1 h. Airdry and LPS groups received either functionalized with Rose Bengal dye or dexamethasone or combination. For CSDEX, tooth was immersed in NPs solution (30 μg/mL, 1 min) and replanted. For CSRB, tooth was immersed in NPs solution (0.1 mg/mL) and light (540 nm) activated to a total dose of 40 J/cm^2 in 1 min [28] and replanted back into the socket. Maxillary left incisor in each rat served as healthy control and rats from same group was caged together. RHR maintained the allocation information on the grouping and EB and AK were blinded about this information during data analysis. To minimize post-operative pain, Buprenorphine SR (1–1.2 mg/kg body weight) was injected subcutaneously for 2 days and mashed food for first week. All rats were followed up till 21 days and no rats were excluded from the experiment. Rats were euthanized in CO_2 chamber and maxillary jaw was dissected for micro-CT analysis. For TRAP and immunofluorescence staining, samples were fixed in 10 % neutral formalin for 24h. Samples were treated with 12.5 % EDTA until complete decalcification, and exposed to sequential dehydration (70 %, 95 %,100 %), xylene, and embedded in paraffin wax. 5 μm thick serial cross sections of tooth with surrounding PDL and bone were obtained. Following deparaffination and sequential rehydration, sections were incubated with commercially available TRAP stain (# 386A, Sigma-Aldrich, St. Louis MO) for 1 h at 37 °C. Total TRAP+ multinucleatedcells (MNC) were counted for each sample and mean ± SD was presented for each group. Immunofluorescence staining for assessment of periostin and osteocalcin was performed similar to protocol to followed for the 3D model. Slides were scanned with Zeiss Axio Scan.Z1 (CamiLod, Toronto, ON, Canada) at × 40 objective. Fluorescence intensity for stain was measured and normalized to area using Zeiss Zen 3.7.

3. Statistical analysis

Data were analysed using GraphPad Prism software (Version 8.0.1; GraphPad, La Jolla, CA) One way ANOVA with Tukey's multiple comparison test. Data are presented as mean ± standard deviation ($p < 0.05$).

4. Results

4.1. Immunofluorescence analysis

Characterization of 3D model: The collagen-based 3D PDLF- Mϕ model consisted of core 3D PDLF construct surrounded by Mϕ with total diameter 3.8 mm ± 0.3 and thickness 300–500 μm.

Mϕ polarization: NPs downregulated CD80 and upregulated CD206 significantly at both early and late phase (Fig. 2A-D). In the early phase, resorptive group showed greater reduction in CD80 with CSNP than CSDEX and inflammatory group and combination group showed greater reduction of CD80 with CSDEX than CSNP. In the late phase, CSDEX showed lower CD80 expression than CSNP in all the groups. Decreased CD80 expression with CSDEX compared to CSNP was highly significant in inflammatory group followed by combination group. Both NPs upregulated CD206 expression in a linear fashion from early to late phase. CSNP showed greater upregulation of CD206 than CSDEX with highest upregulation in resorptive group, followed by combination and inflammatory group.

Multinucleation markers: NPs significantly reduced NFATc1 and STAT6 at both early and late phase (Fig. 2E–H). During early phase, CSDEX reduced NFATc1 much more than CSNP in resorptive and combination group. In the late phase, both NPs showed similar degree of NFATc1 reduction. Both NPs showed similar reduction in STAT6 at early phase. In late phase, CSNP showed higher reduction of STAT6 than CSDEX in inflammatory and resorption group.

Periostin: CSNP showed greater periostin expression than CSDEX in early phase (Fig. 2I–J) particularly in inflammatory and combination group. In the late phase, CSDEX groups showed higher periostin expression than CSNP particularly in inflammatory and resorption group.

4.2. Cytokines and protease analysis

NPs downregulated TNF-α levels with a greater reduction observed in CSDEX than CSNP in the early phase (Fig. 3A). Highest reduction of TNF-α with CSDEX treatment was observed in inflammatory group and combination group. In late phase, both NPs showed similar degree of reduction in the TNF-α. IL6 levels were upregulated with NPs treatment, specifically higher in CSNP than CSDEX in the early phase (Fig. 3B). While both NPs showed higher IL6 than groups without NPs in late

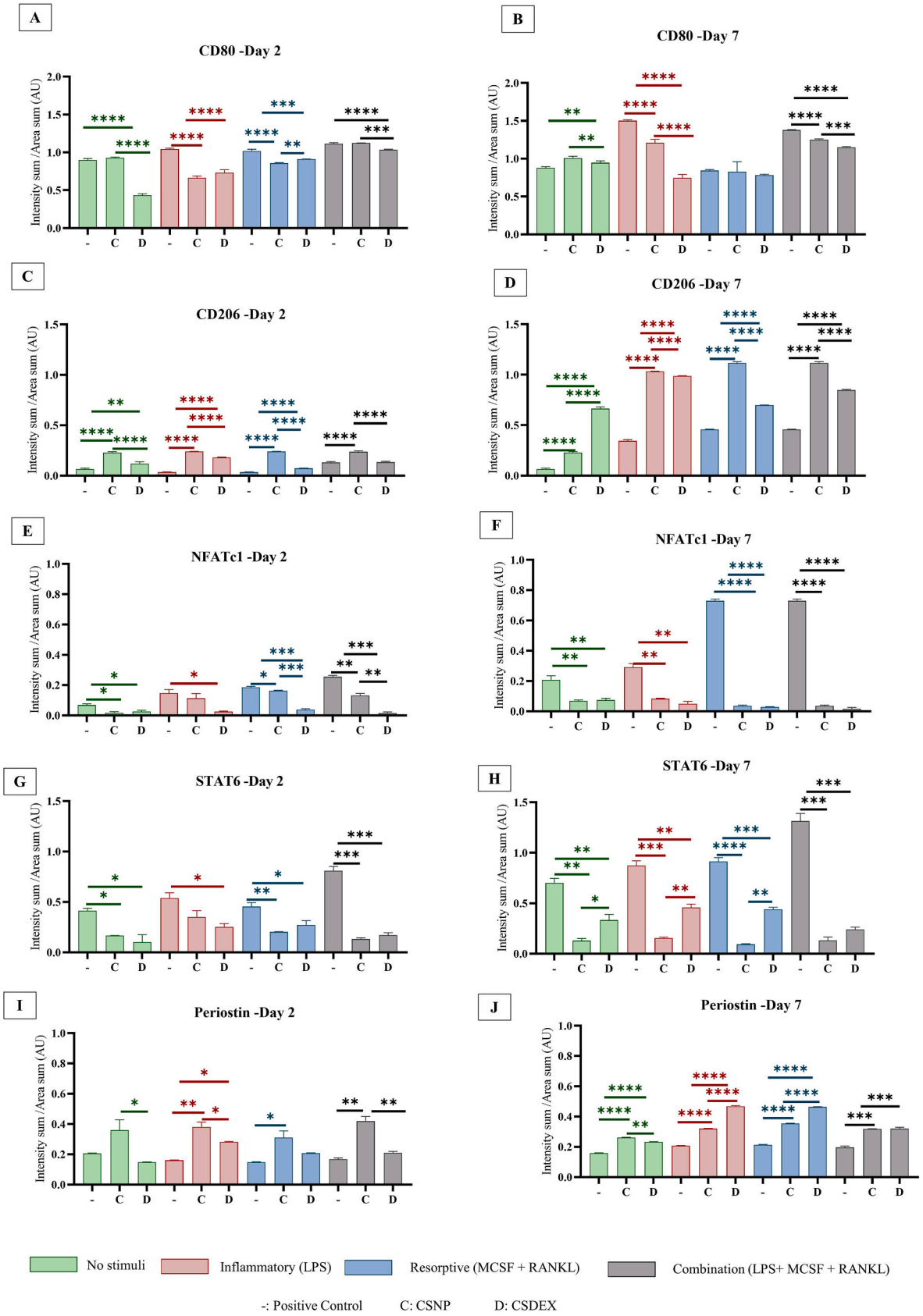

Fig. 2. Immunofluorescence analysis of PDLF-Mϕ 3D coculture model showing Mϕ markers (CD80 (A–B), CD206 (C–D), NFATc1 (E–F), STAT6(G–H) and Periostin (I–J) on day 2 and day 7 in groups without nanoparticles, CSNP and CSDEX treated groups. Data from each experimental stimuli with and without nanoparticles analysed using with One way ANOVA with Tukey's multiple comparison test. *$p < 0.05$ and $^{\geq}$***$p < 0.0001$.

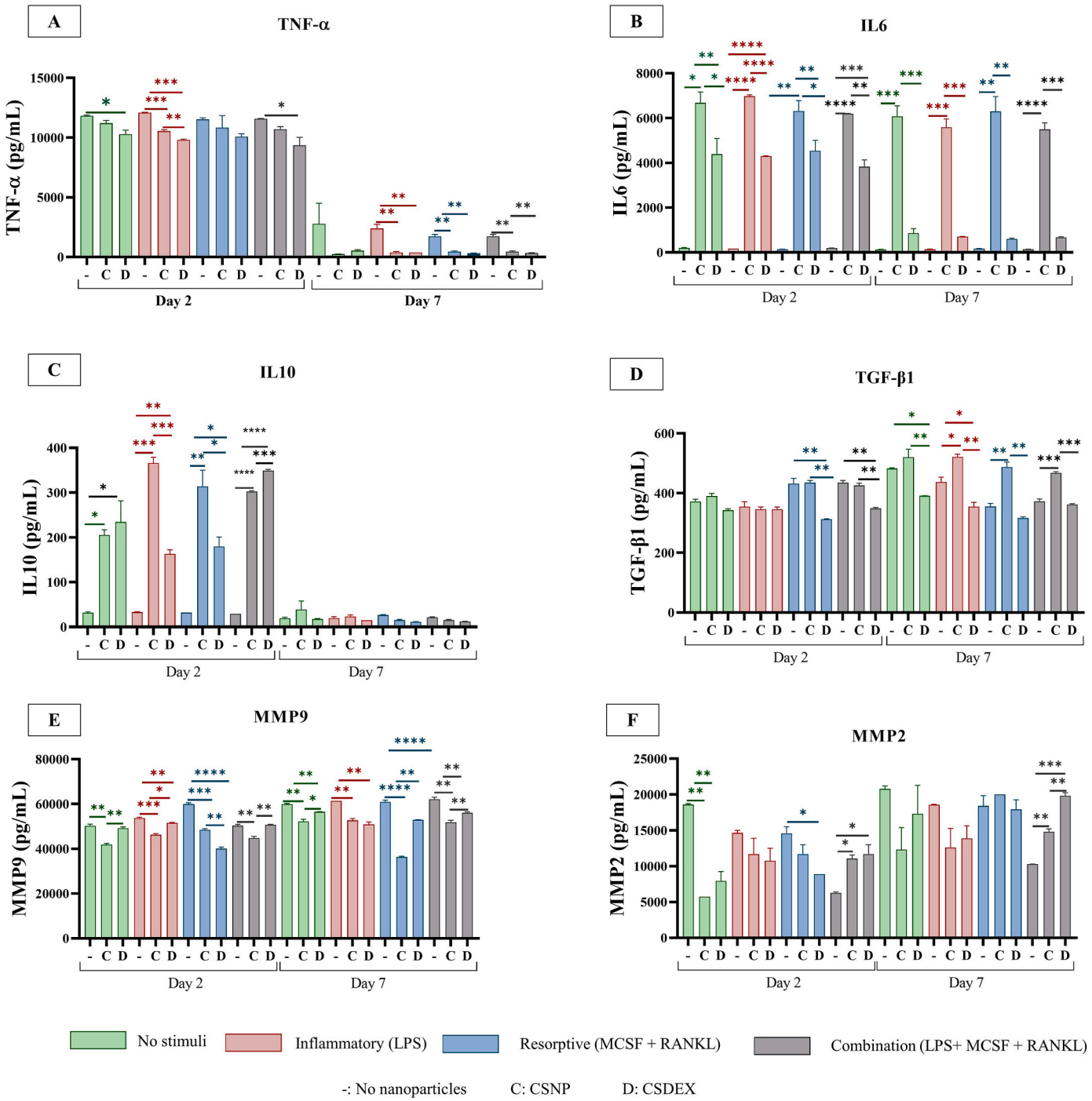

Fig. 3. Cytokines (A–D) and MMPs (E and F) assessment from the cell culture supernatant collected on day 2 and day 7 from PDLF-Mϕ 3D coculture model exposed to different experimental stimuli with or without nanoparticles (CSNP, CSDEX). Data was analysed using with One way ANOVA with Tukey's multiple comparison test. $^{*}p < 0.05$, and $^{\geq ***}p < 0.0001$.

phase, the difference was statistically significant only with CSNP. IL10 levels were substantially increased by both NPs only in early phase (Fig. 3C). CSNP increased IL10 in inflammatory and resorptive group, and CSDEX in combination group. TGF-β1 was significantly upregulated only in the late phase with CSNP (Fig. 3D). NPs treatment showed significant reduction in the MMP9 levels (Fig. 3E) in both early and late phase. During early phase, lower MMP9 was observed with CSNP in inflammatory and combination group and with CSDEX in resorptive group (Fig. 3E). In late phase, CSNP predominantly reduced MMP9 levels in resorptive and combination group and CSDEX reduced MMP9 significantly in inflammatory group. NPs downregulated the MMP2 (Fig. 3F) expression in inflammatory and upregulated in combination group during both early and late phase. In resorptive group, MMP2 levels were downregulated in early phase in CSDEX group and no difference in late phase.

4.3. Animal study

4.3.1. Micro-computed tomography

Samples were imaged in three dimensions using a Bruker Sky-Scan1272 micro-CT scanner (Mouse Imaging Centre - The Centre for Phenogenomics, The Hospital for Sick Children, Toronto, ON, Canada),

with the X-ray source of 100 kV and 100 mA, 360° rotation at 0.3-degree intervals, generating 1200 projections at a resolution of 11 μm per voxel. The middle region of root apicocoronally of root (400 μm) excluding apical and cervical part was chosen for analysis of area of resorption and ankylosis. Sections at every 20th Z plane were included for analysis and each section was divided into four quadrants and assessed for areas of resorption and ankylosis (Fig. 4A). Highest area of resorption and ankylosis was observed in airdry group followed by LPS and then PBS (Fig. 4B–D). CSDEX/CSRB treated groups showed significant reduction in resorption and ankylosis in both Airdry and LPS groups. Among the NPs, lowest area of resorption was observed in CSDEX + CSRB < CSRB < CSDEX. A similar pattern was observed for ankylosis (Fig. 4C and D). In LPS stimuli category, CSRB and CSDEX + CSRB combination groups did not show any ankylosis.

4.3.2. TRAP staining

CSDEX/CSRB treated groups showed significantly lower number of TRAP $^{+ve}$ MNC compared to Airdry, LPS and PBS (Fig. 5A–B). In airdry stimuli, the lowest number of TRAP $^{+ve}$ MNC was observed in CSDEX + CSRB < CSRB < CSDEX (Fig. 5A–B). In LPS stimuli, all NPs showed a similar reduction in TRAP $^{+ve}$ MNC.

4.3.3. Immunofluorescence analysis

CSDEX/CSRB treated groups significantly downregulated osteocalcin expression and upregulated periostin compared to airdry and LPS alone (Fig. 6A-D). Osteocalcin in Airdry + CSDEX, LPS + CSDEX, LPS + CSRB was similar to PBS and LPS + CSRB, Airdry + CSDEX + CSRB and LPS + CSDEX + CSRB was similar to healthy control (Fig. 6C). Lowest periostin was observed in Airdry followed by LPS. Periostin in LPS + CSDEX, Airdry + CSRB, LPS + CSRB, was similar to PBS and periostin in Airdry + CSDEX + CSRB, LPS + CSDEX + CSRB and LPS + CSDEX was similar to healthy control (Fig. 6D).

5. Discussion

The study developed collagen-based 3D PDLF-Mϕ model to simulate microenvironment of root resorption following traumatic dental avulsion, and to understand the treatment effect of engineered nanoparticles in these micro-environments. The stage-wise 3D model development offers the advantage of placing PDLF in a collagen matrix simulating the core of a healthy periodontium in stage one, which is then invaded by immune cells depicted by the introduction of Mϕ along with inflammatory/resorptive stimuli in stage two to simulate the microenvironment. Type I collagen, a predominant collagen type of PDL was used as matrix to simulate cellular interaction via juxtracrine, paracrine and cell-matrix interaction observed in in-vivo state (Fig. 7A). 3D model thickness is comparable to PDL thickness range 150–380 μm [39]. *P gingivalis* derived LPS is a potent endotoxin that stimulate proinflammatory mediators from PDLF and macrophages favoring clastic differentiation of osteoclastic precursors [33]. While MCSF is essential for the survival of osteoclastic precursors, RANKL directs them to differentiate to osteoclasts [5]. Thus, the developed model serves as an ideal model to simulate cellular interactions in root resorption. In the animal study, extracted teeth were either air dried or treated with LPS for 1 h [33,38] to simulate the tissue response following traumatic dental injury [40].

In the literature, $Ca(OH)_2$ has been used in the management of inflammatory root resorption owing to its ability to increase the pH of dentin (8.0–10.0) thereby inhibiting osteoclast mediated acid hydrolase activity besides activating alkaline phosphatase [41]. Hydroxyl group is responsible for the alkaline environment which imparts antibacterial property and stimulates necrosis of resorptive lesions, and calcium ions are suggested to activate calcium dependent adenosine triphosphatase associated with hard tissue formation. However it is suggested that $Ca(OH)_2$ should be used with caution due to its necrotizing effect on the cells repopulating the root surface which in turn would increase the risk of ankylosis [41]. The combination of antibiotic-corticosteroid intracanal medication have been used with a rationale to reduce the inflammation in the periodontal membrane via inhibiting odontoclasts and detaching them from the damaged root surface [42]. Lower number of teeth have been shown to have ankylosis with Ledermix four out of twelve) compared $Ca(OH)_2$ (nine out of fifteen) with differences being statistical non-significant [43].

Root dentin is a highly mineralized bio-composite material with its organic and inorganic phases together which provides optimal strength to the tooth [21]. Dentin matrix displays both intrafibrillar and interfibrillar component in which intrafibrillar mineralization exists within gap zones of collagen fibrils, and interfibrillar mineralization occurs in interstitial spaces between fibrils [44]. Due to this complex hierarchical structure, restoration of the dentin matrix following arresting resorption remains challenging with the conventional strategies.

Osteoclastic differentiation is a complex process which starts from macrophage polarization, multinucleation followed by expression of proteases to degrade root structure [7]. Hence in the current study, therapeutic effect of engineered nanoparticles was assessed in stage wise manner by determining Mϕ polarization, multinucleation, cytokines and protease expression. While both CSNP and CSDEX downregulated CD80, they demonstrated temporal activity. CSNP was most effective during the early phase and CSDEX in the late phase. In contrast, similar level of upregulation of CD206 was observed in both CSNP and CSDEX in a linear fashion from early to late phase with upregulation of anti-inflammatory phenotype. Multi-nucleation is one of the critical steps in clastic differentiation of Mϕ and previous studies have shown positive role of NFATc1 and STAT6 in this process [5,15]. Both CSNP and CSDEX showed similar reduction of NFATc1, whereas CSNP was more effective in reducing STAT6 when compared to CSDEX.

To further understand cellular molecules involved in the CSNP and CSDEX mediated immunomodulation of Mϕ polarization and multinucleation, cytokine profiling was performed. Proinflammatory cytokine TNFα was effectively reduced, with higher reduction in CSDEX compared to CSNP highlighting higher anti-inflammatory activity of CSDEX validating the reduction in M1 phenotype. Increased IL6 with CSNP and CSDEX was an interesting data observed in the current study. Functional pleiotropy is a characteristic feature of cytokines and growth factors [45]. IL6 although primarily known to be pro-inflammatory cytokine, it has been found to have regenerative and anti-inflammatory functions [45]. IL6 classical signalling has been shown to have positive role in the activation of STAT3-mediated pathways which induced regeneration of intestinal epithelial cells and hepatocytes [46,47]. Higher IL-6 secretion in CSNP-treated biofilm has been observed which might have also mediated the increased IL-10 production [27]. Considering the overall result with reduction in clastic activity with CSNP and CSDEX treatment, it can be suggested that increased IL6 in the current experimental setup had less of pro-inflammatory role and greater inclination towards protective role. To further support anti-inflammatory effects of the nanopartciles, IL10 was significantly upregulated with CSNP and CSDEX primarily in the early phase and this finding is in line with the previous studies of biofilm treated PDLF-Mϕ indirect coculture system exposed to CSNP [14,27]. MMP9, an osteoclast specific protease [48,49] has been found to be the most upregulated protease associated with root resorption. MMP9 was downregulated substantially in the current study with a greater reduction observed in CSNP than CSDEX. MMP2 was upregulated by both CSNP and CSDEX only in combination group with higher effect observed in CSDEX.

Matricellular protein periostin plays a crucial role in collagen fibrillogenesis and tissue integrity by causing proteolytic activation of lysyl-oxidase during collagen crosslinking [50]. Periostin expression was upregulated by CSNP throughout the interaction phases, and effect of CSDEX was observed during the late phase. Sustained higher periostin upregulation by CSNP could be attributed to its ability to increase TGFβ1 (50). Airdry group in animal model showed lowest periostin (Fig. 6D)

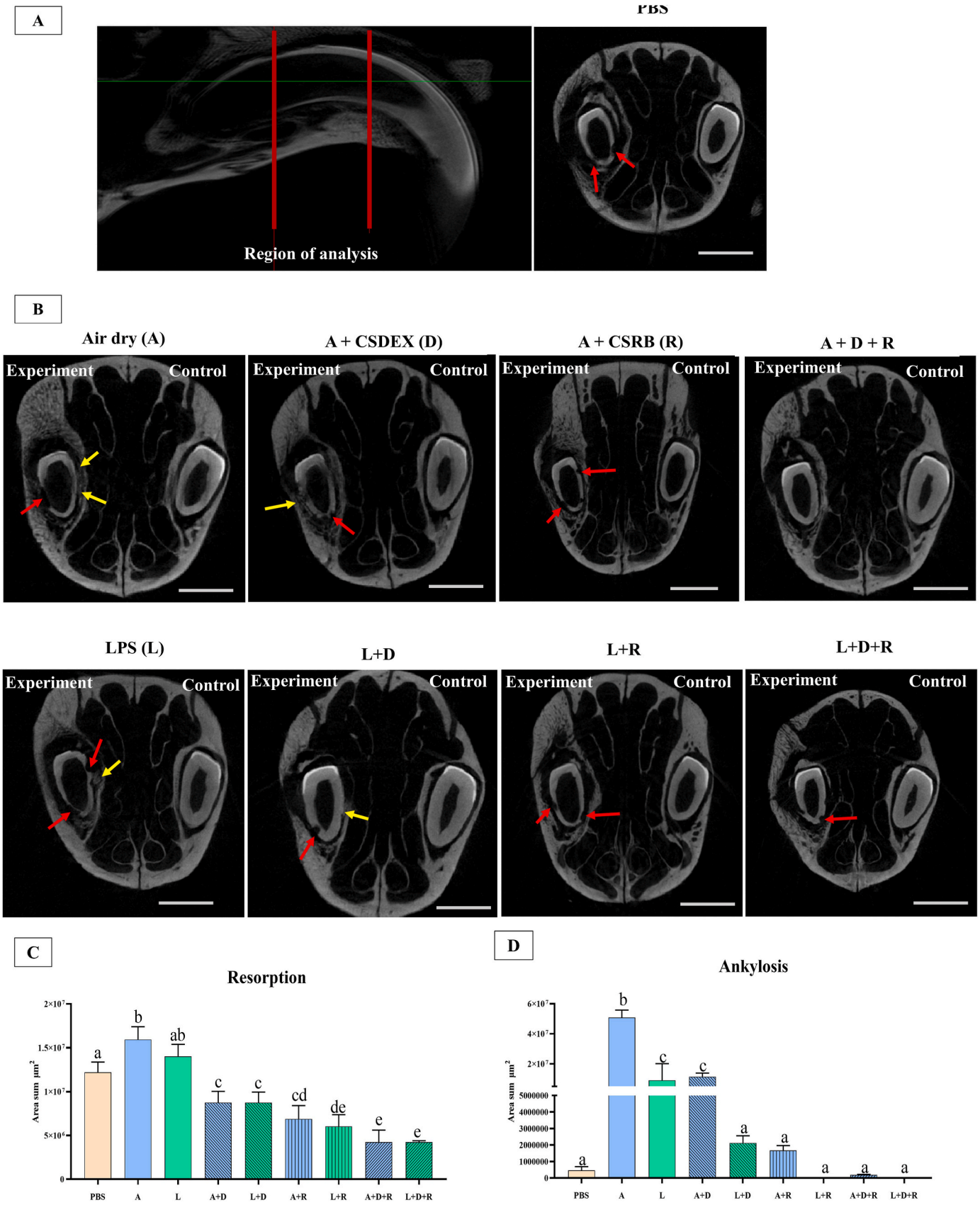

Fig. 4. (A) shows micro-CT image depicting apico-coronal extension of region of interest selected for analysis and cross-sectional view of tooth PBS group depicting the division of section into four quadrants for analysis. Fig. 3B representative micro-CT images and figure C and D shows quantification of resorption and ankylosis respectively. Red and yellow arrows indicate areas of resorption and ankylosis respectively. Data was analysed using with One way ANOVA with Tukey's multiple comparison test. Different alphabets indicate the difference observed is statistically significant $p < 0.0001$. Scale Bar: 2000 µm.

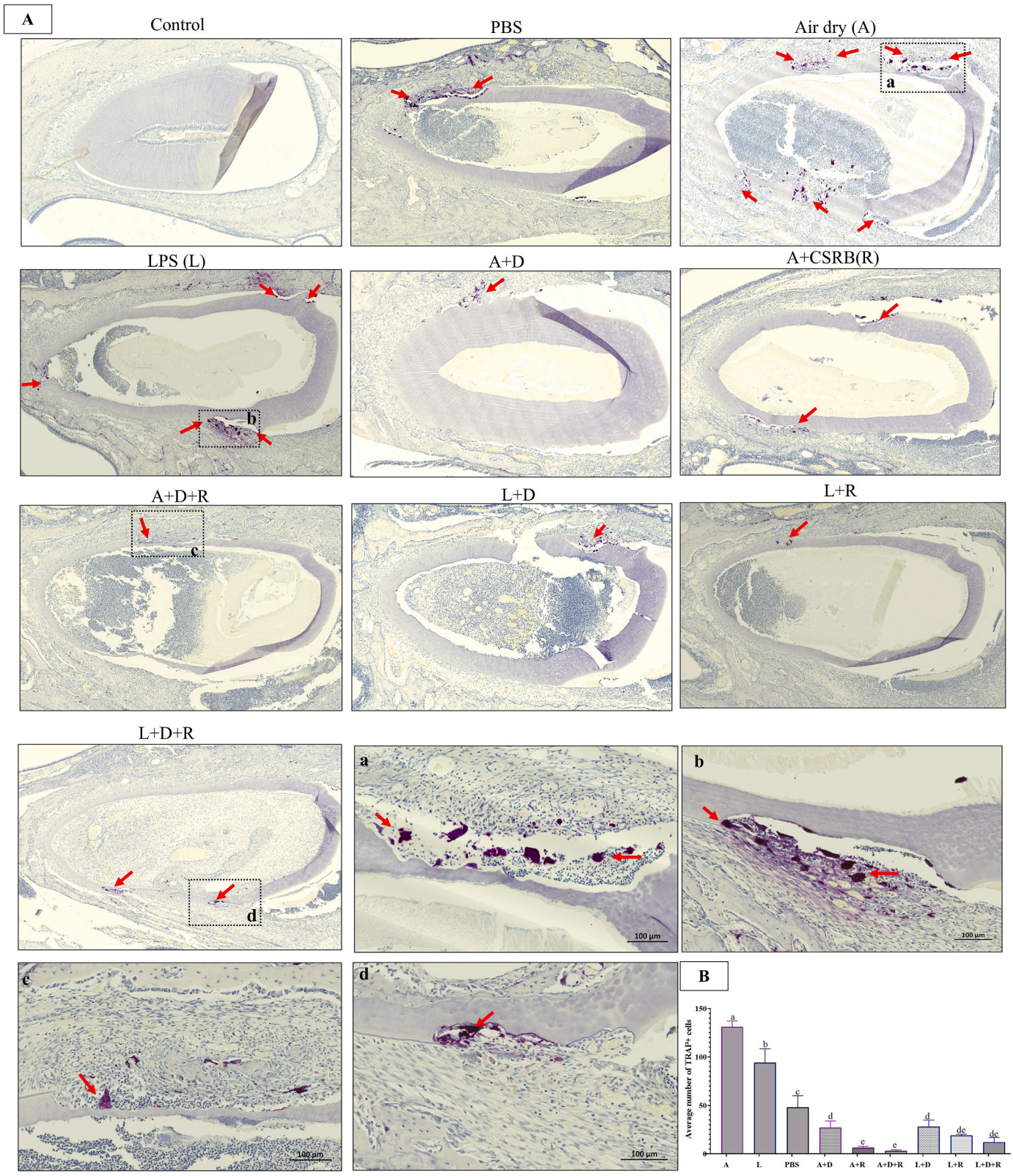

Fig. 5. A and B shows representative images of TRAP $^{+}$ multinucleated cells (MNC) and quantitative data respectively. Specific regions (dotted rectangles) of Airdry (a), LPS (b), Airdry + CSDEX + CSRB (c) and LPS + CSDEX + CSRB (d) shows higher magnification of TRAP^{+} MNC. Data was analysed using with One way ANOVA with Tukey's multiple comparison test. Different alphabets indicate the difference observed is statistically significant $p < 0.0001$.

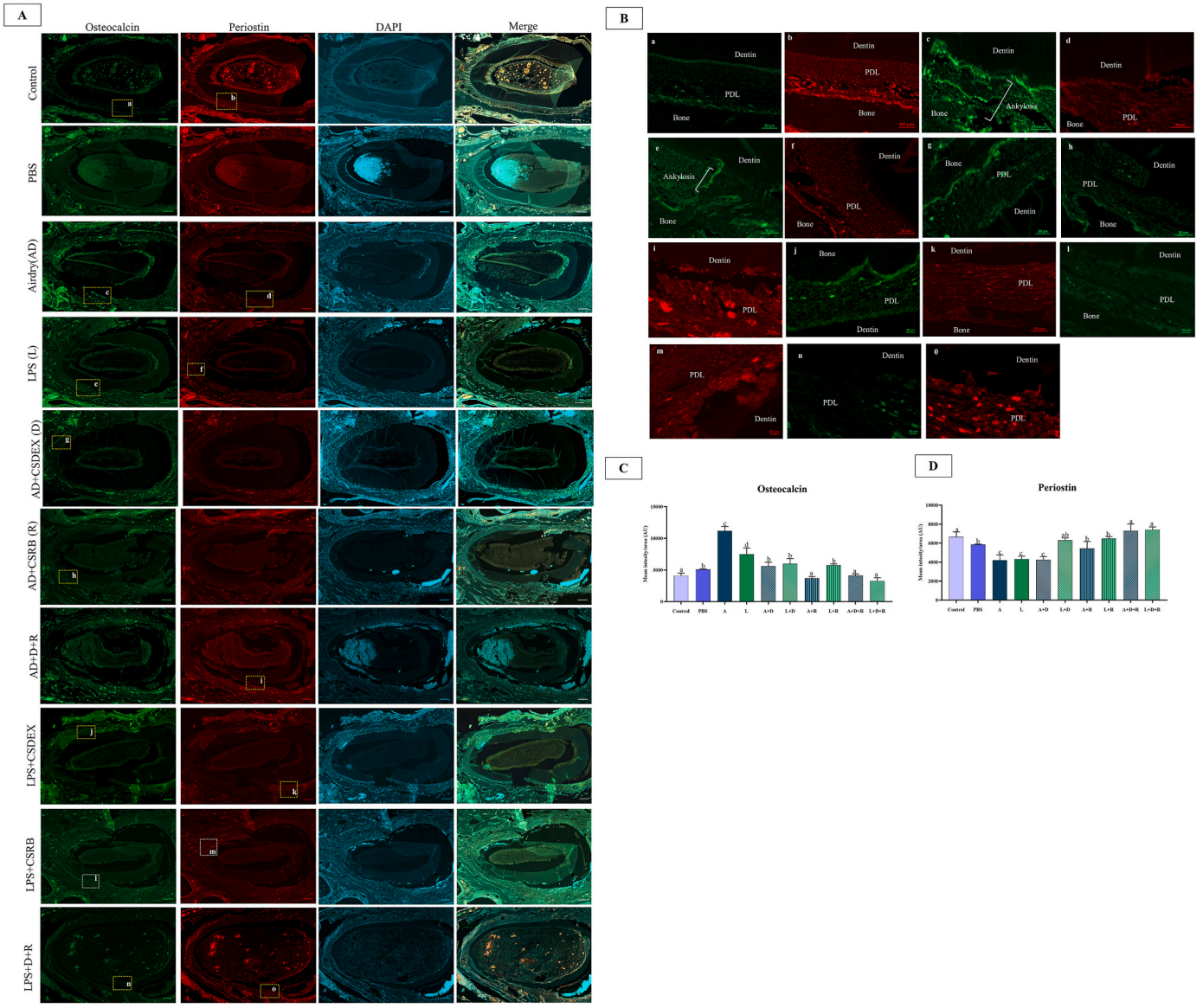

Fig. 6. (A) shows representative images of immunofluorescence analysis of osteocalcin and periostin expression (Scale bar 200 μm). (B) represents higher magnification of the selected regions from images from A. Quantification of osteocalcin and periostin expression are shown in C and D respectively. Data was analysed using with One way ANOVA with Tukey's multiple comparison test. Different alphabets indicate the difference observed is statistically significant $p < 0.0001$.

and highest osteocalcin expression in the regions of ankylosis (Fig. 6C). While both CSDEX and CSRB group downregulated osteocalcin and upregulated periostin, observation was significantly effective when used in combination (Fig. 6 i and o). CSDEX/CSRB mediated increased periostin expression, thus favouring PDLF cell proliferation and attachment on the root surface. Furthermore, the expression of periostin can enhance the adhesion of osteoblasts while simultaneously impeding their migration [51]. This finding explains the effectiveness of the tested engineered bioactive nanoparticles in inhibiting ankylosis.

Periostin is a crucial extracellular matrix protein expressed by periodontal ligament fibroblasts. It regulates homeostasis, maintains periodontal tissue integrity, and is involved in repairing damage caused by external stimuli. Periostin also plays a role in cell adhesion, collagen formation, and tissue regeneration. Its expression is primarily detected in the fibroblasts of the periodontal ligament and the osteoblasts of the alveolar bone. The increased expression of periostin in the CSRB treated group may indicate a cellular response from periodontal fibroblasts and reparative activities in the PDL tissues [52]. Micro-CT analysis and the reduction of TRAP + ve MNC in animal models exposed to airdry or LPS further supported these findings. An overview of engineered bioactive nanoparticles guided modulation of cellular crosstalk in the 3D PDLF-Mϕ model is presented in Fig. 7B. In the current study, root surface biomodification with CSRB effectively prevented root resorption and ankylosis by stabilizing the extracellular matrix. Additionally, CSRB has been found to deactivate bacterial LPS even in the presence of tissue fluids, reduced the exaggerated proinflammatory response, and promoted macrophage polarization to an anti-inflammatory phenotype [29]. The reduction in the resorptive activity following root surface treatment with CSRB with photoactivation is also in line with a recent clinical case report where root surface treatment with photoactivated CSRB arrested resorptive process with clinical improvement [53].

Engineering nanosized immunomodulatory bioactive materials such as chitosan nanoparticles functionalized with photosensitizer and anti-inflammatory agent dexamethasone possesses greater advantages over conventional synthetic agents such as antimicrobial agents, and Ca $(OH)_2$ as this is host immune modulation-based therapy. Immune modulation therapy in the current study is focused on ameliorating the exaggerated response of host response by downregulating the pro-

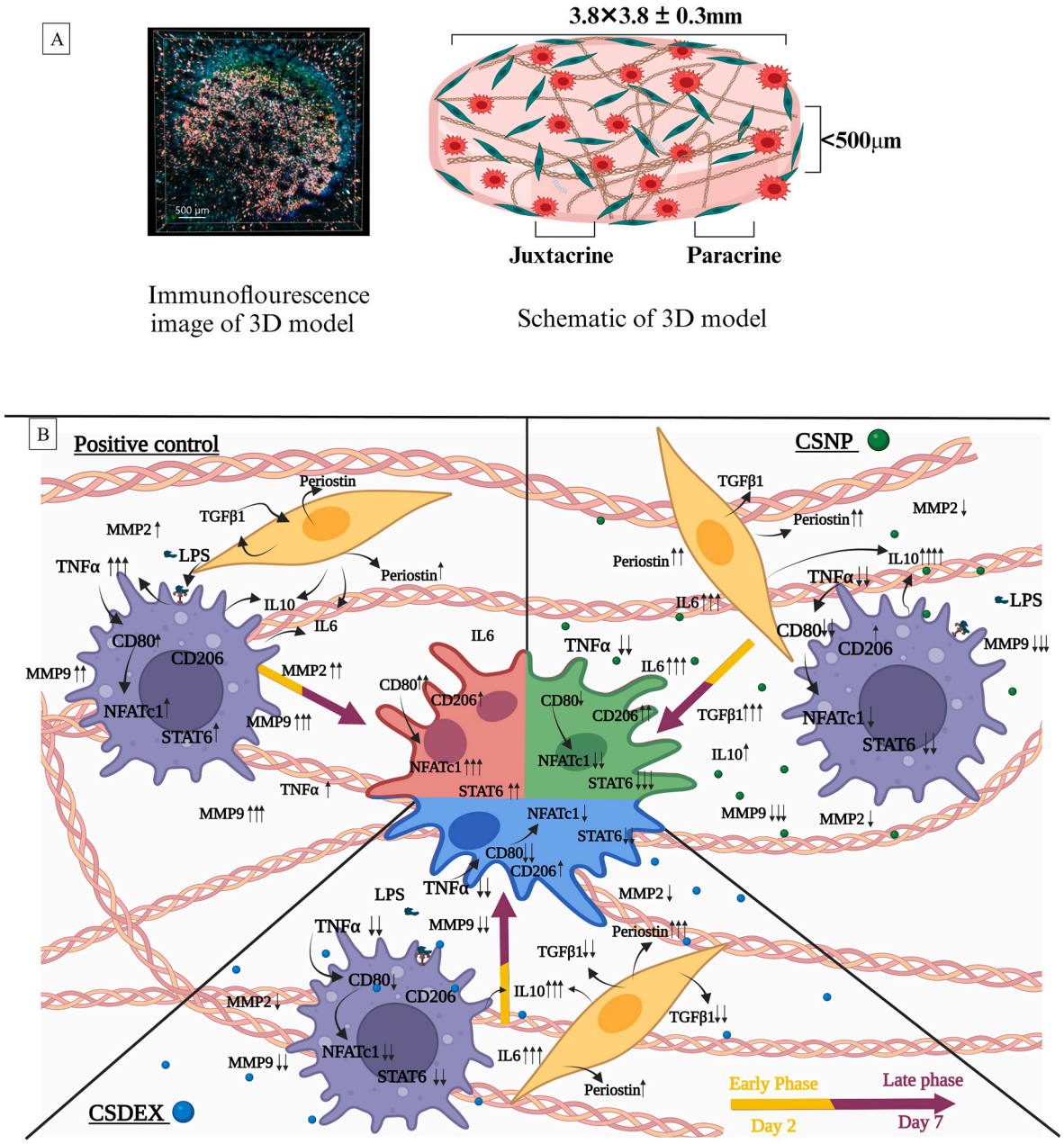

Fig. 7. A represents schematic representation of 3D PDLF-Mϕ model supporting cellular interaction via juxtacrine, paracrine and via matrix. B demonstrated nanoparticles guided PDLF-Mϕ crosstalk modulation in reducing osteoclastic differentiation and resorptive function of Mϕ. 3D PDLF-Mϕ coculture without nanoparticles treatment designated as positive control showed greater levels of osteoclastic differentiation of Mϕ. Coculture showed increased M1 phenotype marker (CD80) and multinucleation activity as represented by NFATc1 and STAT6. Proinflammatory cytokine TNFα, and protease MMP9 were increased while anti-inflammatory cytokine IL10, TGF-β levels were reduced. In contrast, CSNP/CSDEX treated 3D PDLF-Mϕ coculture showed lower osteoclastic differentiation of Mϕ with reduced M1 polarization and multinucleation and upregulation of IL10 and periostin. While both CSNP and CSDEX were effective in the reduction osteoclastic differentiation of Mϕ, they showed temporal and marker specific differences. Different number of upward facing or downward facing arrows shows the difference in their activity with respect to time and the markers.

inflammatory microenvironmental burden on the cells and upregulating anti-inflammatory and enhancing dentin matrix stabilization to achieve favourable healing in avulsed teeth. From the application point, chitosan offers additional advantage owing to its hydrophilic nature that favors the intimate binding to root surface forming a uniform gel like coating on the root surface. CSNP has been found to be effectively internalized via clathrin-mediated endocytosis, macropinocytosis, and phagocytosis subsequent to electrostatic interaction of cationic CSNP with negatively charged plasma membrane [27]. Clathrin coated pits have been observed on the plasma membrane of Mϕ and PDLF as early as 3h after CSNP treatment, followed by appearance of membrane-bound vesicles internalizing CSNP. Membrane protrusions characteristic of macropinocytosis and phagocytosis have been observed at 24h suggesting the uptake of relatively larger particles of CSNP(27). These CSNP have been found to effectively trafficked intracellularly within membrane-bound organelles, endosomes, multivesicular bodies, and lysosomes to execute immune to mediate cellular functions.

5.1. Conclusion

A novel collagen-based 3D heterogenous coculture model simulating cellular interactions in root resorption and an animal model were

employed to study the therapeutic effect of engineered functional bioactive nanoparticles. The engineered photosensitizer functionalized chitosan nanoparticles and sustained dexamethasone-releasing chitosan nanoparticles effectively modulated cellular crosstalk to inhibit Mϕ polarization to M1 phenotype and multinucleation/clastic differentiation. While both NPs efficiently upregulated IL10, CSDEX demonstrated more anti-inflammatory activity via higher downregulation of TNFα and CSNP/CSRB demonstrated a more significant effect on TGFβ1, matricellular protein periostin and downregulated ankylotic marker osteocalcin and MMP9. Engineered bioactive CSDEX/CSRB nanoparticles promoted a favourable periodontal healing environment in traumatized teeth.

Ethics approval and consent to participate

The study protocol was approved by the Ethics Review Board, University of Toronto (#20012802) and protocol follows ARRIVE guidelines 2.0. Human PDLF were provided as a kind gift from Dr. Douglas Hamilton's lab, Schulich's School of Medicine & Dentistry, London, ON, Canada. Cells were isolated from clinical samples of healthy periodontium.

CRediT authorship contribution statement

Rajeshwari Hadagalu Revana Siddappa: Writing – review & editing, Writing – original draft, Methodology, Investigation, Formal analysis, Data curation, Conceptualization. **Emily Bishop:** Writing – review & editing, Methodology, Investigation, Formal analysis, Data curation, Conceptualization. **Aiman Ali:** Writing – review & editing, Methodology, Investigation. **Anil Kishen:** Writing – review & editing, Supervision, Resources, Project administration, Methodology, Investigation, Funding acquisition, Conceptualization.

Declaration of competing interest

The authors declare that they have no known competing financial interests or personal relationships that could have appeared to influence the work reported in this paper.

Acknowledgments

Authors would like to thank Dr. Nanka Dimitrova from Division of Comparative Medicine, University of Toronto, Kimberly Lau from The Imaging Facility at The Hospital for Sick Children, and Adam Gibson from, Analytical Facility of Bioactive Molecules, and Cameron Goddard from The Centre for Phenogenomics The Hospital for Sick Children, Toronto, Ontario, Canada, and Leonardo Alan Delanora Department of Diagnosis and Surgery, School of Dentistry, São Paulo State University (UNESP), Araçatuba, Brazil for their valuable support. The current study was supported in part by a research grant from the American Association of Endodontists Foundation (#1208771), Natural Sciences and Engineering Research Council of Canada (Discovery grant) (AK-RGPIN-2020-05844), Canada Research Chair Program, and Dr. Lloyd and Mrs. Kay Chapman Chairship.

Appendix A. Supplementary data

Supplementary data to this article can be found online at https://doi.org/10.1016/j.bioactmat.2024.07.017.

References

[1] S. Patel, T.P. Ford, Is the resorption external or internal? Dent. Update 34 (4) (2007) 218–220, 22, 24-220, 29.
[2] L. Andersson, J. Friskopp, L. Blomlöf, Fiber-glass splinting of traumatized teeth, ASDC (Am. Soc. Dent. Child.) J. Dent. Child. 50 (1) (1983) 21–24.
[3] M. Trope, Luxation injuries and external root resorption–etiology, treatment, and prognosis, J. Calif. Dent. Assoc. 28 (11) (2000) 860–866.
[4] A.M. Mavridou, E. Hauben, M. Wevers, E. Schepers, L. Bergmans, P. Lambrechts, Understanding external cervical resorption in vital teeth, J. Endod. 42 (12) (2016) 1737–1751.
[5] M. Pereira, E. Petretto, S. Gordon, J.H.D. Bassett, G.R. Williams, J. Behmoaras, Common signalling pathways in macrophage and osteoclast multinucleation, J. Cell Sci. 131 (11) (2018).
[6] D. Sokos, V. Everts, T.J. de Vries, Role of periodontal ligament fibroblasts in osteoclastogenesis: a review, J. Periodontal. Res. 50 (2) (2015) 152–159.
[7] A. Iglesias-Linares, J.K. Hartsfield, Cellular and molecular pathways leading to external root resorption, J. Dent. Res. 96 (2) (2017) 145–152.
[8] C.A. McCulloch, Origins and functions of cells essential for periodontal repair: the role of fibroblasts in tissue homeostasis, Oral Dis. 1 (4) (1995) 271–278.
[9] P.V. Abbott, Prevention and management of external inflammatory resorption following trauma to teeth, Aust. Dent. J. 61 (Suppl 1) (2016) 82–94.
[10] B.D.M. Souza, K.L. Dutra, M.M. Kuntze, E.A. Bortoluzzi, C. Flores-Mir, J. Reyes-Carmona, et al., Incidence of root resorption after the replantation of avulsed teeth: a meta-analysis, J. Endod. 44 (8) (2018) 1216–1227.
[11] L. Blomlöf, S. Lindskog, K.G. Hedström, L. Hammarström, Vitality of periodontal ligament cells after storage of monkey teeth in milk or saliva, Scand. J. Dent. Res. 88 (5) (1980) 441–445.
[12] V. Bloemen, T. Schoenmaker, T.J. de Vries, V. Everts, Direct cell-cell contact between periodontal ligament fibroblasts and osteoclast precursors synergistically increases the expression of genes related to osteoclastogenesis, J. Cell. Physiol. 222 (3) (2010) 565–573.
[13] J. Zhang, X. Liu, C. Wan, Y. Liu, Y. Wang, C. Meng, et al., NLRP3 inflammasome mediates M1 macrophage polarization and IL-1β production in inflammatory root resorption, J. Clin. Periodontol. 47 (4) (2020) 451–460.
[14] H. Hussein, A. Kishen, Engineered chitosan-based nanoparticles modulate macrophage-periodontal ligament fibroblast interactions in biofilm-mediated inflammation, J. Endod. 47 (9) (2021) 1435–1444.
[15] H.R.S. Rajeshwari, A. Kishen, Periodontal fibroblasts-macrophage crosstalk in external inflammatory root resorption, J. Endod. (2023).
[16] A. Sainio, H. Järveläinen, Extracellular matrix-cell interactions: focus on therapeutic applications, Cell. Signal. 66 (2020) 109487.
[17] S.A. Langhans, Three-dimensional, Front. Pharmacol. 9 (2018) 6.
[18] S. Zhu, S. Ehnert, M. Rouß, V. Häussling, R.H. Aspera-Werz, T. Chen, et al., From the clinical problem to the basic research-Co-culture models of osteoblasts and osteoclasts, Int. J. Mol. Sci. 19 (8) (2018).
[19] G. Tsilingaridis, B. Malmgren, C. Skutberg, O. Malmgren, The effect of topical treatment with doxycycline compared to saline on 66 avulsed permanent teeth–a retrospective case-control study, Dent. Traumatol. 31 (3) (2015) 171–176.
[20] A. Filippi, Y. Pohl, T. von Arx, Treatment of replacement resorption with Emdogain–preliminary results after 10 months, Dent. Traumatol. 17 (3) (2001) 134–138.
[21] M. Behnaz, S.S. Izadi, F. Mashhadi Abbas, O. Dianat, S. Sadeghabadi, T. Akbarzadeh, et al., The impact of platelet-rich fibrin (PRF) on delayed tooth replantation: a preliminary animal study, Aust. Endod. J. 47 (3) (2021) 457–466.
[22] K.Y. Kum, O.T. Kwon, L.S. Spängberg, C.K. Kim, J. Kim, M.I. Cho, et al., Effect of dexamethasone on root resorption after delayed replantation of rat tooth, J. Endod. 29 (12) (2003) 810–813.
[23] A. Lengheden, L. Blomlöf, S. Lindskog, Effect of immediate calcium hydroxide treatment and permanent root-filling on periodontal healing in contaminated replanted teeth, Scand. J. Dent. Res. 99 (2) (1991) 139–146.
[24] M. Esposito, M.G. Grusovin, N. Papanikolaou, P. Coulthard, H.V. Worthington, Enamel matrix derivative (Emdogain(R)) for periodontal tissue regeneration in intrabony defects, Cochrane Database Syst. Rev. (4) (2009) CD003875.
[25] A. Shrestha, M.R. Hamblin, A. Kishen, Photoactivated rose bengal functionalized chitosan nanoparticles produce antibacterial/biofilm activity and stabilize dentin-collagen, Nanomedicine. 10 (3) (2014) 491–501.
[26] M.N. Kumar, R.A. Muzzarelli, C. Muzzarelli, H. Sashiwa, A.J. Domb, Chitosan chemistry and pharmaceutical perspectives, Chem. Rev. 104 (12) (2004) 6017–6084.
[27] H. Hussein, A. Kishen, Proteomic profiling reveals engineered chitosan nanoparticles mediated cellular crosstalk and immunomodulation for therapeutic application in apical periodontitis, Bioact. Mater. 11 (2022) 77–89.
[28] A. Shrestha, S. Friedman, C.D. Torneck, A. Kishen, Bioactivity of photoactivated functionalized nanoparticles assessed in lipopolysaccharide-contaminated root canals in vivo, J. Endod. 44 (1) (2018) 104–110.
[29] K. Singh, A. Ali, A. Shrestha, M. Magalhaes, A. Kishen, Assessing macrophage polarization in nanoparticle-guided wound repair using a lipopolysaccharide contaminated intraosseous model, J. Endod. 48 (1) (2022) 109–116.
[30] F.C. Li, A. Kishen, Microtissue engineering root canal dentine with crosslinked biopolymeric nanoparticles for mechanical stabilization, Int. Endod. J. 51 (10) (2018) 1171–1180.
[31] V. Sae-Lim, Z. Metzger, M. Trope, Local dexamethasone improves periodontal healing of replanted dogs' teeth, Endod. Dent. Traumatol. 14 (5) (1998) 232–236.
[32] S. Shrestha, A. Diogenes, A. Kishen, Temporal-controlled dexamethasone releasing chitosan nanoparticle system enhances odontogenic differentiation of stem cells from apical papilla, J. Endod. 41 (8) (2015) 1253–1258.
[33] L. Gölz, S. Memmert, B. Rath-Deschner, A. Jäger, T. Appel, G. Baumgarten, et al., LPS from P. gingivalis and hypoxia increases oxidative stress in periodontal ligament fibroblasts and contributes to periodontitis, Mediat. Inflamm. 2014 (2014) 986264.

[34] A.E. Kasonga, V. Deepak, M.C. Kruger, M. Coetzee, Arachidonic acid and docosahexaenoic acid suppress osteoclast formation and activity in human CD14+ monocytes, in vitro, PLoS One 10 (4) (2015) e0125145.
[35] Souzani A. Mahdi, H.R.S. Rajeshwari, P.R. Selvaganapathy, A. Kishen, Impact of 3D collagen-based model and hydrostatic pressure on periodontal ligament fibroblast: a morpho-biochemical analysis, J. Mech. Behav. Biomed. Mater. 147 (2023) 106092.
[36] A. Shrestha, Z. Shi, K.G. Neoh, A. Kishen, Nanoparticulates for antibiofilm treatment and effect of aging on its antibacterial activity, J. Endod. 36 (6) (2010) 1030–1035.
[37] S. Shrestha, A. Kishen, Temporal-controlled bioactive molecules releasing core-shell nano-system for tissue engineering strategies in endodontics, Nanomedicine 18 (2019) 11–20.
[38] L.A.B. da Silva, D.L. Longo, M.B.S. Stuani, A.M. de Queiroz, R.A.B. da Silva, P. Nelson-Filho, et al., Effect of root surface treatment with denusomab after delayed tooth replantation, Clin. Oral Invest. 25 (3) (2021) 1255–1264.
[39] A. Nanci, D.D. Bosshardt, Structure of periodontal tissues in health and disease, Periodontol 40 (2000. 2006) 11–28.
[40] L. Hammarström, L. Blomlöf, S. Lindskog, Dynamics of dentoalveolar ankylosis and associated root resorption, Endod. Dent. Traumatol. 5 (4) (1989) 163–175.
[41] L. Tronstad, J.O. Andreasen, G. Hasselgren, L. Kristerson, I. Riis, pH changes in dental tissues after root canal filling with calcium hydroxide, J. Endod. 7 (1) (1981) 17–21.
[42] G.S. Heithersay, Management of tooth resorption, Aust. Dent. J. 52 (1 Suppl) (2007) S105–S121.
[43] P.F. Day, T.A. Gregg, P. Ashley, R.R. Welbury, B.O. Cole, A.S. High, et al., Periodontal healing following avulsion and replantation of teeth: a multi-centre randomized controlled trial to compare two root canal medicaments, Dent. Traumatol. 28 (1) (2012) 55–64.
[44] A.S. Deshpande, P.A. Fang, X. Zhang, T. Jayaraman, C. Sfeir, E. Beniash, Primary structure and phosphorylation of dentin matrix protein 1 (DMP1) and dentin phosphophoryn (DPP) uniquely determine their role in biomineralization, Biomacromolecules 12 (8) (2011) 2933–2945.
[45] J. Scheller, A. Chalaris, D. Schmidt-Arras, S. Rose-John, The pro- and anti-inflammatory properties of the cytokine interleukin-6, Biochim. Biophys. Acta 1813 (5) (2011) 878–888.
[46] R. Li, D. Li, Y. Nie, IL-6/gp130 signaling: a key unlocking regeneration, Cell Regen. 12 (1) (2023) 16.
[47] H. Qin, L. Wang, T. Feng, C.O. Elson, S.A. Niyongere, S.J. Lee, et al., TGF-beta promotes Th17 cell development through inhibition of SOCS3, J. Immunol. 183 (1) (2009) 97–105.
[48] K. Sundaram, R. Nishimura, J. Senn, R.F. Youssef, S.D. London, S.V. Reddy, RANK ligand signaling modulates the matrix metalloproteinase-9 gene expression during osteoclast differentiation, Exp. Cell Res. 313 (1) (2007) 168–178.
[49] S. Lee, S.J. Bush, S. Thorne, N. Mawson, C. Farquharson, G.T. Bergkvist, Transcriptomic profiling of feline teeth highlights the role of matrix metalloproteinase 9 (MMP9) in tooth resorption, Sci. Rep. 10 (1) (2020) 18958.
[50] A. Kudo, Periostin in fibrillogenesis for tissue regeneration: periostin actions inside and outside the cell, Cell. Mol. Life Sci. 68 (19) (2011) 3201–3207.
[51] T. Cobo, C.G. Viloria, L. Solares, T. Fontanil, E. González-Chamorro, F. De Carlos, et al., Role of periostin in adhesion and migration of bone remodeling cells, PLoS One 11 (1) (2016) e0147837.
[52] H.Y. Xu, E.M. Nie, G. Deng, L.Z. Lai, F.Y. Sun, H. Tian, et al., Periostin is essential for periodontal ligament remodeling during orthodontic treatment, Mol. Med. Rep. 15 (4) (2017) 1800–1806.
[53] N. Suresh, H.J. Subbarao, V. Natanasabapathy, A. Kishen, Maxillary anterior teeth with extensive root resorption treated with low-level light-activated engineered chitosan nanoparticles, J. Endod. 47 (7) (2021) 1182–1190.